# Hydroxypropyl-β-Cyclodextrin Copolymers and Their Nanoparticles as Doxorubicin Delivery System

TIEWEI WANG,[1] CHUNLING ZHANG,[2] XING-JIE LIANG,[1] WEI LIANG,[2] YAN WU[1]

[1]Laboratory for Biological Effects of Nanomaterials and Nanosafety, National Center for Nanoscience and Technology, Chienese Academy of Sciences, Beijing 100190, China

[2]National Laboratory of Biomacromolecules, Institute of Biophysics, Chinese Academy of Sciences, Beijing 100101, China

*Received 8 February 2010; revised 26 August 2010; accepted 28 August 2010*

*Published online 4 October 2010 in Wiley Online Library (wileyonlinelibrary.com). DOI 10.1002/jps.22352*

**ABSTRACT:** A novel biodegradable amphiphilic copolymer composed of hydroxypropyl-β-cyclodextrin, polylactide, and 1,2-dipalmitoyl-sn-glycero-3-phosphoethanolamine, was successfully synthesized. The chemical structures of copolymers were determined by FT-IR, $^{1}$H nuclear magnetic resonance (NMR) spectroscopy, $^{13}$C NMR, $^{31}$P NMR, thermogravimetric analysis ,and differential scanning calorimetry. Doxorubicin (DOX)-loaded copolymer nanoparticles (NPs) were prepared by double emulsion and nanoprecipitation methods. The factors of copolymer composition and fabrication methods, which influence size and encapsulation efficiency (EE) were investigated. Their EE to DOX could reach 90.6% at an available condition. *In vitro* release behavior of NPs showed a continuous release after a burst release. The antitumor activity of the DOX-loaded NPs against cancer HepG2 and A549 cells was evaluated by 3-(4, 5-dimethylthiazol-2-yl)-2,5-diphenyl tetrazolium bromide method. The DOX-loaded copolymer NPs showed comparable anticancer efficacy with the free drug. © 2010 Wiley-Liss, Inc. and the American Pharmacists Association J Pharm Sci 100:1067–1079, 2011

**Keywords:** HP-β-CD; polylactide; 1; 2-dipalmitoyl-sn-glycero-3-phosphoethanolamine; amphiphilic copolymer; doxorubicin; delivery system; antitumor activity

## INTRODUCTION

Amphiphilic copolymers consisting of hydrophilic and hydrophobic segments can form micelle structures with hydrophobic inner core and hydrophilic outer shell in aqueous media. It was clearly shown that micelles possess a number of unbeatable advantages as potential drug delivery systems for poorly soluble pharmaceuticals.[1,2] The hydrophobic core of micelles may be used as a cargo space for encapsulation of a variety of sparingly soluble therapeutic and diagnostic agents. Such encapsulation substantially increases their bioavailability, protects them from destructive factors upon parenteral administration, and beneficially modifies their pharmacokinetics and biodistribution.[1,2] The size of micelles permits their extravasation and accumulation in a variety of pathological sites, where the permeability of the vascular endothelium is increased, such as infarct zones and tumors.[3–6] This fact provides a unique opportunity for physiology-based targeting of drugs and/or drug-loaded pharmaceutical carriers, such as micelles, to these pathological areas via the enhanced permeability and retention (EPR; or "passive" targeting) effect.[7,8] An additional advantage of micelles as drug carriers, from the practical application view, is that they are easy to prepare on a large scale.

A number of pharmaceutical micelle-forming compounds with low toxicity and high solubilization power are currently available. Conventional surfactants, however, have critical micelle concentration (CMC) values in a millimolar range and may dissociate upon being diluted to therapeutically acceptable concentrations. *In vivo*, this may result in micelle collapse in a large blood volume with a subsequent precipitation of the encapsulated drug, that is, sharp decrease in its bioavailability and ability to penetrate biological barriers.[2]

As has been known, in aqueous media, certain polyethylene glycol–phosphatidylethanolamine

*Correspondence to*: Chunling Zhang (Telephone: +86-10-648-453-88; Fax: +86-10-648-453-88; E-mail: zhangcl@moon.ibp.ac.cn); Yan Wu (Telephone: +86-10-82545614; Fax: +86-10-82545614; E-mail: wlingw66@sina.com)

These institutions contributed equally to this work.

Journal of Pharmaceutical Sciences, Vol. 100, 1067–1079 (2011)

(PEG–PE) conjugates form very stable micelles. The PEG-based corona makes these micelles long-circulating, whereas the lipid hydrophobic core may be used as a cargo space for poorly soluble compounds, including many anticancer drugs.[9–11] The characteristic size, stability, and the longevity in the systemic circulation make PEG–PE micelles a promising carrier for the delivery of drugs to the ill site via the EPR effect.[12,13] But the PEG–PE copolymers are expensive and this will hinder its further applications.

Cyclodextrins (CDs) are a series of polyhydroxy compounds consisting of six to eight D-glucopyranose residues linked by α-1,4-glycosidic bonds into a macrocycle. Many CD derivatives have been synthesized as novel drug carriers to extend the physicochemical properties and inclusion capacity of natural CDs.[14,15] The CDs and modified CDs are often used as the promising excipients for the stability of drug during the fabrication of microspheres and nanoparticles (NPs).[16–19] In addition, high encapsulation efficiency (EE) could be achieved because of the inclusion ability of the CD moieties in the copolymers. It was found that CDs and their derivatives could bind drug via the formation of inclusion complexes.[20]

Doxorubicin (DOX), a well known anticancer drug, is a member of the anthracycline ring antibiotics, with a broad spectrum of antitumor activity, including a variety of human and animal solid tumor. However, its therapeutic potential has been restricted by its dose-limited cardiotoxicity and myelosuppression.[21–23] The result of this is often a narrow therapeutic index, due to high levels of toxicity to healthy tissues.

In this paper, we designed and synthesized a novel biodegradable amphiphilic copolymer, hydroxypropyl-β-cyclodextrin-polylactide-1,2-dipalmitoyl-sn-glycero-3-phosphoethanolamine (HP-β-CD-PLA-DPPE). The copolymers consisted of hydrophilic, HP-β-CD, segment and hydrophobic, PLA and DPPE, segment. The copolymers were characterized on the basis of FT-IR, $^{1}$H NMR, $^{13}$C NMR, and $^{31}$P NMR measurements. The DOX-loaded copolymer NPs were fabricated by double emulsion (DE) and nanoprecipitation (NP) methods. The morphological examination of NPs was performed using transmission electron microscope (TEM) and scanning electron microscopy (SEM). Here, a comparative study based on their physicochemical characteristics, drug release, and anticancer activities has also been performed.

## MATERIALS AND METHODS

### Materials

Hydroxypropyl-β-cyclodextrin (HP-β-CD) and D, L-lactide (DLLA) were obtained from Alfa Aesar (Ward Hill, Massachusetts), $Sn(Oct)_2$, 4-dimethylaminopyridine, DPPE, triethylamine,

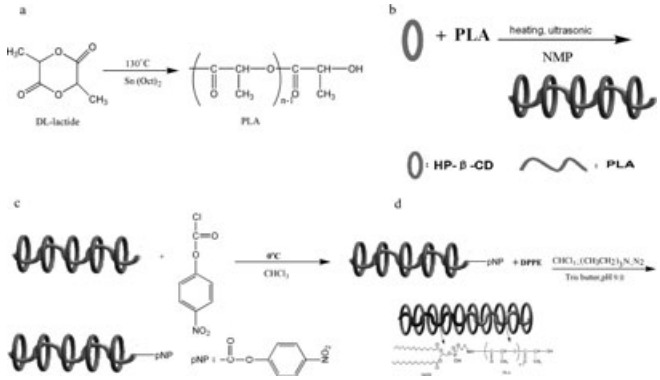


**Scheme 1.** (a) The synthesis route of PLA, (b) HP-β-CD-PLA inclusion complex, (c) HP-β-CD -PLA-pNP copolymer, and (d) HP-β-CD-PLA-DPPE copolymer.

4-nitrophenyl chloroformate, 4-dimethylaminopyridine (DMAP), N-methyl-2-pyrrolidone (NMP), polyvinyl alcohol (PVA;13,000–23,000 g/mol),and doxorubicin hydrochloride were purchased from HaiZheng Corp. (Taizhou, Zhenjiang, China). All other reagents and solvents were of analytical grade.

### Synthesis of PLA and HP-β-CD-PLA Inclusion Complex

PLA was synthesized (Scheme 1a) at 120°C in 12 h through a ring opening polymerization procedure of DLLA sealed in an ampoule in the presence of $Sn(Oct)_2$, as described previously.[24] The product was dissolved with chloroform and then precipitated with cold methanol. The purified copolymers were dried at 40°C for 48 h in a vacuum oven. The average molecular weight (Mw) of the final product was 10 kDa, which was measured by gel permeation chromatography (GPC) using polystyrene as standard.

HP-β-CD-PLA inclusion complex (Scheme 1b) was synthesized by solution-ultrasonic technique, as described previously,[25,26] with some modifications. Briefly, PLA (200 mg, Mw = 10 kDa) was dissolved in 10 mL of NMP and then mixed with 2.5 g of HP-β-CD at 80°C. After initial stirring for 0.5 h, the solution was ultrasonically agitated for another 4 h, and then cooled to 4°C. The solution was then dialyzed for 24 h and freeze-dried. Finally, the product was dried continuously at 60°C in vacuum for 12 h.

### Synthesis of HP-β-CD-PLA-pNP

Several activation methods for polymer containing hydroxyl have been considered: tosylation,[27,28] esterification using 4-nitrophenyl chloroformate,[29,30] carbonyl diimidazole,[31] cyanogen halide,[32] and so on. In our work, 4-nitrophenyl chloroformate was selected for the activation of hydroxyl groups of HP-β-CD-PLA. The activation of HP-β-CD-PLA inclusion complex (HP-β-CD-PLA-pNP) (Scheme 1c) was performed as follows: first, 1.2 g of HP-β-CD-PLA inclusion complex was dissolved in 3 mL of chloroform. 0.5 g of

 DOI 10.1002/jps

4-nitrophenyl carbonate and 0.02 g of DMAP were dissolved in a mixture of 3 mL chloroform and 3 mL pyridine. Then, the mixture was added stepwise to the above reaction flask containing HP-β-CD-PLA at 0°C, and continued stirring for 8 h using DMAP as a catalyst. The chloroform was finally evaporated under reduced pressure to 1 mL. The obtained products were precipitated with the mixture of petroleum and ether (1:1, v/v), and washed by the mixture of petroleum and ether three times to remove catalyst and unreacted chloroformate.

### Synthesis of HP-β-CD-PLA-DPPE Copolymers

The reaction of HP-β-CD-PLA-pNP and DPPE as reported previously,[33] is performed with with slight modification. Briefly, 1.0 g of HP-β-CD-PLA-pNP was dissolved in 3 mL of chloroform. 0.1 g of DPPE was dissolved in 3 mL chloroform with 200 μL triethylamine. Then, the solution of DPPE was added stepwise to the HP-β-CD-PLA-pNP reaction flask, and the sample was incubated at room temperature with stirring under $N_2$. After being stirred continuously for 12 h, the organic solvents were removed using a rotary evaporator. The obtained HP-β-CD-PLA-pNP-DPPE copolymer was purified using reverse phase high pressure liquid chromatography preparative column with methanol or 0.01 M HCl (70/30, v/v) as a mobile phase, and the mobile phase was removed by the vacuum evaporator. The purified HP-β-CD-PLA-pNP-DPPE copolymer was stored as a powder at −20°C.

To prepare HP-β-CD-PLA-DPPE copolymer (Scheme 1d) and remove the pNP group, the HP-β-CD-PLA-pNP-DPPE copolymer above-mentioned was added to Tris buffer (pH 9.0), then mixed and incubated overnight at 4°C under an argon atmosphere. The obtained HP-β-CD-PLA-DPPE copolymer was purified by overnight dialysis against distilled water at 4°C using a dialysis bag (Mw cut-off= 8000 g/mol), after which samples were freeze-dried. HP-β-CD-PLA-DPPE copolymer was identified by NMR and stored as a powder at −20°C.

### Characterization of the Chemical Structure of HP-β-CD and HP-β-CD-PLA-DPPE Copolymer

The structure of the samples were confirmed through FT-IR (Perkin-Elmer, Waltham, Massachusetts) and pressed to a plate with KBr. The scanning range was from 4000 to 500 $cm^{-1}$.

The NMR ($^1$H-NMR, $^{13}$C-NMR, $^{31}$P-NMR) was recorded on an NMR spectrometer (Bruker AVANCE 400, Ettlingen,Baden-Württemberg, Germany). During the measurement, HP-β-CD was dissolved in dimethyl sulfoxide (DMSO)-*d6* and HP-β-CD-PLA-DPPE copolymers were dissolved in $CdCl_3$.

The GPC was performed on a Waters 2410 GPC apparatus (Milford, Massachusetts). Mw and Mw distribution of the copolymers were calculated using polystyrene as the standard.

The thermal stability of samples was measured using thermogravimetric analysis (TGA; Perkin-Elmer, Waltham, Massachusetts). The temperature range was carried out from 25°C to 900°C under nitrogen flow with heating rate of 20°C/min. The thermoproperty of samples was also measured using differential scanning calorimeter (DSC). Samples (3–5 mg) were loaded into aluminum pans and the DSC thermograms were recorded on a Pyris Diamond DSC apparatus (Perkin-Elmer, Waltham, Massachusetts). To observe the glass transition temperature ($T_g$) , all of the DSC thermograms were obtained with a heating procedure during which, by using nitrogen flow, the heating rate reached 10°C/min in the range of 25°C–230°C.

### Biodegradation of HP-β-CD-PLA-DPPE Copolymer

Biodegradation of the copolymers was carried as follows: 20 mg samples of the copolymers were compressed with a mold into a film on a Carver Laboratory Press (Fred S. Carver Inc., Wabash, Indiana) at room temperature. Biodegradation (%)=$100(W_1\text{-}W_d)/W_1$, Where $W_1$ and $W_d$ represent the dried weight of the original film and the weight after incubating in phosphate buffer saline (PBS; pH 7.4) at 37°C for specific days), respectively.

### Preparation of Dox-Loaded HP-β-CD-PLA-DPPE Copolymer Nanoparticles

The DOX-loaded HP-β-CD-PLA-DPPE copolymer NPs were prepared by DE and NP methods.[34,35] Briefly, for the DE method, the HP-β-CD-PLA-DPPE copolymer (50 mg) was dissolved in 3 mL dichloromethane, and 500 μL of DOX (1 mg/mL) aqueous solution ($W_1$) was added to the copolymer solution. The mixture was emulsified by sonication for 1 min (13 W) in an ice-bath. Then, 2 mL of 2 % (w/v) PVA solution ($W_2$) was added and sonicated for 30 s to make a $W_1$/O/$W_2$ double emulsion. The double emulsion was diluted into 20 mL PVA solution (0.3 %, w/v) and dichloromethane was evaporated under reduced pressure in a rotary evaporator. Finally, the obtained DOX-loaded NPs were collected by centrifugation at 13,000g for 10 min and then washed three times with deionized water, before lyophilization.

For the NP method, the HP-β-CD-PLA-DPPE copolymer (20 mg) was dissolved in 3 mL acetone, and the copolymer solution was added drop by drop to 20 mL of distilled water with 100 μL DOX (1 mg/mL) at a rate of 0.5 mL/min using a syringe pump (74,900 series multichannel syringe pumps, Cole-Parmer Instrument Company, Vernon Hills, Illinois), under magnetic stirring for 10 min, and acetone was evaporated under reduced pressure. The obtained DOX-loaded NPs were collected by

centrifugation at 13,000g for 10 min and then washed three times with deionized water before lyophilization.

The EE was determined by measuring the DOX concentration in the supernatant obtained after centrifugation of NPs using ultra-violet (UV) absorbance at 490 nm. The EE was calculated by the following equation:

$$EE\% = 100 \times (W_o - W_t)/W_o$$

where, $W_o$ and $W_t$ were the weights of initial amount of DOX and that of DOX detected in supernatant after centrifuging twice, respectively. Each sample was assayed in triplicate.

### Characterization of HP-β-CD-PLA-DPPE and Dox-Loaded HP-β-CD-PLA-DPPE Nanoparticles

Nanoparticle sizes and ζ potential were determined using a Zetasizer Nano series ZEN 3600 (Malvern Instruments Ltd., Worcestershire, UK). The experiment was performed at a wavelength of 633 nm with a constant angle of 90° at 25°C using the samples, appropriately diluted with distilled water. For ζ potential, the sample was diluted with a 0.05 M NaCl solution to a constant ionic strength.

The morphology of the plain NPs was performed using a TEM (Hitachi, H-600,Tokyo, Japan). Before visualization, a droplet of nanoparticle suspension containing 2 % (w/w) phosphotungstic acid was placed on copper grid and dried.

SEM (Hitachi, S-4800,Tokyo, Japan) was used to observe the morphology of drug-loaded NPs. A drop of nanoparticle solution was deposited onto a silicon chip and air-dried before SEM observation.

### *In Vitro* Release Experiment

Five miligrams of lyophilized DOX-loaded HP-β-CD-PLA-DPPE NPs was directly immersed into 30 mL of PBS solution (pH 7.4, 1 mol/L). *In vitro* drug release profile of NPs was determined by loading 1 mL of original nanoparticle solution into dialysis tubing (Mw = 12,000), which was submerged into 10 mL PBS (pH 7.4), and shaken at 37°C, 100 rpm in a water bath. The released drug was retrieved at predetermined time points, and analyzed by using UV absorbance at 490 nm. Each experiment was repeated thrice and the result was the mean value of three samples.

### Cell Culture

Human non-small cell lung carcinoma (A549) cells and Human hepatocellular carcinoma cells (HepG2) were purchased from American Type Culture Collection (ATCC; Manassas, Virginia). Cell culture medium and fetal bovine serum were from Invitrogen (Carlsbad, California). Culture flasks and dishes were from Corning (Corning, New York). Cells were cultured in RPMI 1640 medium or DMEM medium supplemented with 10% heat-inactivated fetal bovine serum, penicillin (100 U/mL), and streptomycin (100 U/mL).

### Analysis of Cytotoxicity

The tumor cells were plated at a density of $5 \times 10^3$ cells/well in 100 μL RPMI-1640 medium in 96-well plates and grown for 24 h. The cells were then exposed to a series of concentrations of free DOX or DOX-loaded NPs for 48 h, and the viability of cells was measured using the methylthiazoletetrazolium method. Briefly, 100 μL of methylthiazoletetrazolium solution (0.5 mg/mL in PBS) was added to each well. The plates were incubated for 4 h at 37°C. After the incubation, 100 μL of DMSO (Sigma-Aldrich, St. Louis, MO, USA) was added to each well for 10 min at room temperature. Absorbance was measured at 570 nm using a plate reader (Thermo, Erlangen, Germany). The mean percentage of cell survival, relative to that of untreated cells and 95% confidence intervals (CIs), were estimated from data from the three individual experiments. The concentration of DOX at which cell killing was 50% was calculated by curve fitting using SPSS software (version 12.0, SPSS Inc., Chicago, Illinois).

### Quantification of Doxorubicin Internalization

To measure the internalization of DOX quantitatively, tumor cells were cultured on 6-well plates for 24 h to achieve approximately 80% confluence. DOX-loaded NPs, free DOX, and empty nanoparticles (DOX concentration, if present, 1 μM; HP-β-CD-PLA-DPPE 7 and 16 mg/mL) were then added to designated wells. After incubation for specific times, the cells were collected for measurement of DOX fluorescence. The fluorescence from individual cells was detected with a flow cytometer (FACSCalibur, BD, San Jose, California). For detection of DOX-derived fluorescence, excitation was with the 488 nm line of an argon laser, and emission fluorescence between 564 and 606 nm was measured. For all experiments in which the intracellular DOX was quantified using flow cytometry, at least 10,000 cells were measured from each sample.

### Statistical Analysis

The data are expressed as mean ± SD. Statistical comparisons were made by *t*-test. $P < 0.05$ was considered significant.

## RESULTS AND DISCUSSION

### Synthesis and Characterization of HP-β-CD-PLA-DPPE Copolymers

The synthesis of the amphiphilic HP-β-CD-PLA-DPPE involves four steps, as shown in Scheme 1.

HP-β-CD-PLA inclusion complex was synthesized by solution-ultrasonic technique (the inclusion complex yield 70%). In our work, 4-nitrophenyl chloroformate was selected for the activation of hydroxyl groups of HP-β-CD-PLA. The degree of carbonate substitution could be determined easily by UV analysis after alkaline hydrolysis. The content of 4-nitrophenyl carbonate moieties was determined during the course of the reaction. The degree of 4-nitrophenyl carbonate substitution was controlled by adjusting the amount of chloroformate added. The degree of substitution initially increased to reach a maximum value at 8 h (43%).

HP-β-CD-PLA-DPPE copolymer was synthesized by the reaction of activated HP-β-CD-PLA (HP-β-CD-PLA-pNP) and DPPE, and finally removing the pNP group in Tris buffer (pH 9.0). The Mw of the HP-β-CD-PLA-DPPE copolymer was controlled by the feed weight ratio of DPPE to HP-β-CD-PLA-pNP. The different samples, namely the HP-β-CD-PLA-DPPE 50:1 (feed weight ratio of DPPE/HP-β-CD-PLA-pNP 1:50), HP-β-CD-PLA-DPPE 30:1 (feed weight ratio of DPPE/HP-β-CD-PLA-pNP 1:30) and HP-β-CD-PLA-DPPE 10:1 (feed weight ratio of DPPE/HP-β-CD-PLA-pNP 1:10), respectively, were synthesized.

The molecular weights and polydispersity index of the HP-β-CD-PLA-DPPE copolymers are shown in Table 1. The amount of DPPE introduced to HP-β-CD-PLA inclusion complex increased with the feed ratio of DPPE to HP-β-CD-PLA-pNP. This indicated that higher the content of DPPE, the higher is the opportunity for DPPE to react with HP-β-CD-PLA-pNP reactive center. The final products of HP-β-CD-PLA-DPPE have good solubility in $CHCl_3$, dimethylformamide, and DMSO.

Figures 1a–1d show the FT-IR spectra of the HP-β-CD, HP-β-CD-PLA, HP-β-CD-PLA-pNP, and HP-β-CD-PLA-DPPE samples, respectively. Compared with HP-β-CD (Fig. 1a), HP-β-CD-PLA (Fig. 1b), HP-β-CD-PLA-pNP (Fig. 1c), and HP-β-CD-PLA-DPPE (Fig. 1d) copolymers have a new absorption peak appearing around 1754 $cm^{-1}$, corresponding to the C=O stretching vibration. Compared with HP-β-CD-PLA (Fig. 1b), HP-β-CD-PLA-pNP (Fig. 1c) showed that the band at 3080 $cm^{-1}$ was corresponding to the −OH bending vibration. Compared with HP-β-CD-PLA-pNP (Fig. 1c), HP-β-CD-PLA-DPPE (Fig. 1d) showed that the band at 2730 $cm^{-1}$ was corresponding to the P−OH stretching vibration. These changes of FT-IR spectra indicated the change in HP-β-CD after the introduction of PLA and DPPE.

**Table 1.** Composition and Molecular Weight Distribution of HP-β-CD-PLA-DPPE Copolymers

| Copolymer | Molecualr Weight of Copolymer[a] | | Polydispersity ($M_w/M_n$) |
|---|---|---|---|
| | $M_w$(kDa) | $M_n$(kDa) | |
| HP-β-CD-PLA-DPPE (50: 1) | 23 | 14 | 1.64 |
| HP-β-CD-PLA-DPPE (30:1) | 31 | 22 | 1.41 |
| HP-β-CD-PLA-DPPE (10:1) | 38 | 25 | 1.52 |

[a] $M_w$ and $M_n$ were measured by gel permeation chromatography.
HP-β-CD-PLA-DPPE, hydroxypropyl-β-cyclodextrin-polylactide-1,2-dipalmitoyl-sn-glycero-3-phosphoethanolamine.

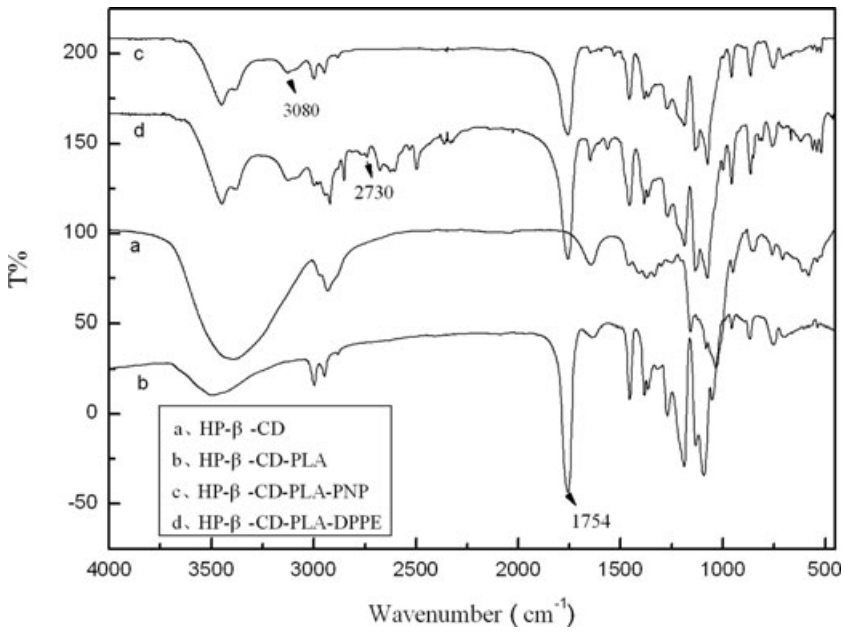


**Figure 1.** Fourier transform infrared spectroscopy spectra of (a) HP-β-CD, (b) HP-β-CD-PLA, (c) HP-β-CD-PLA–pNP, and (d) HP-β-CD-PLA-DPPE (30:1).

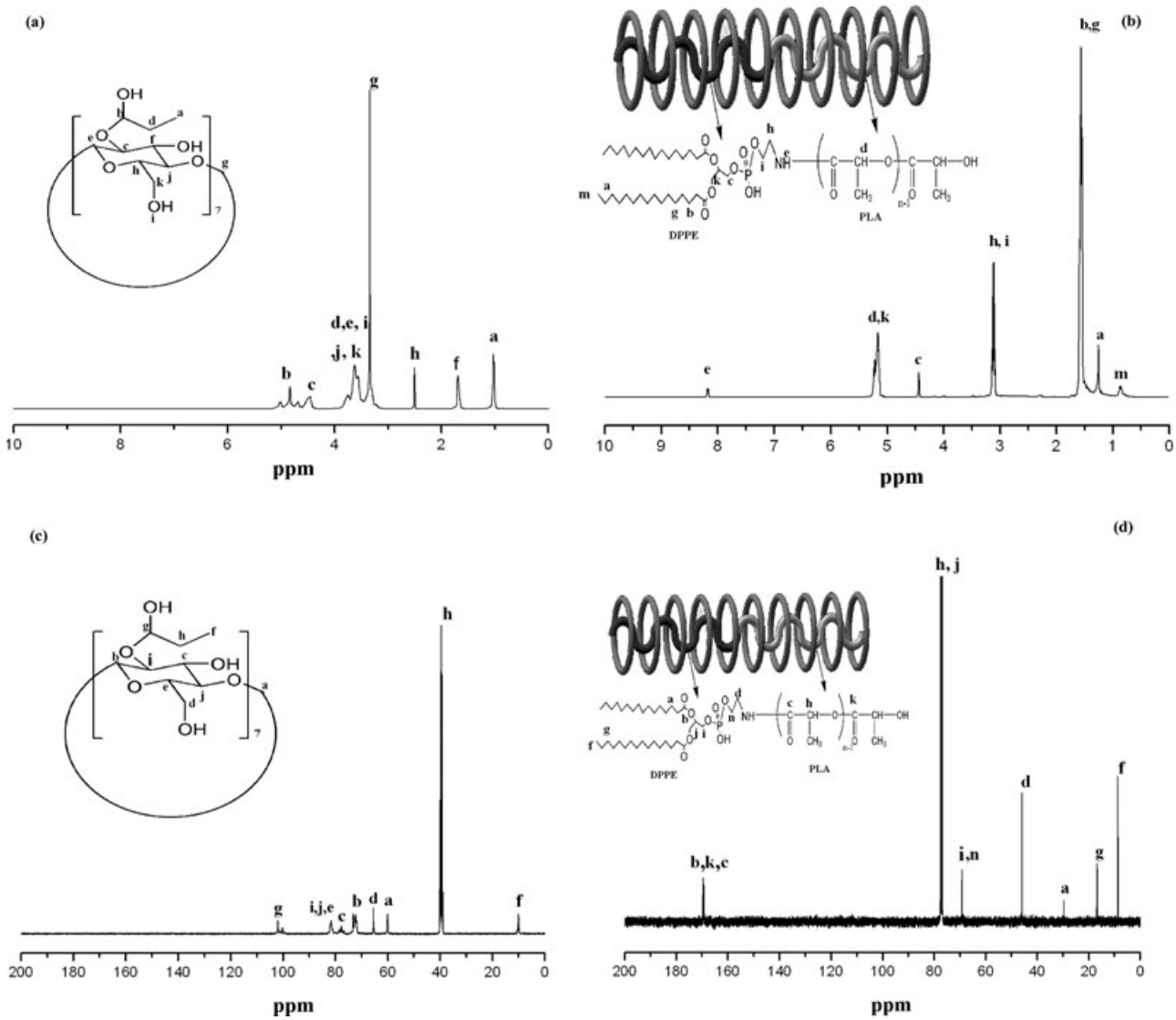


**Figure 2.** $^{1}$H nuclear magnetic resonance (NMR) spectrum of (A) HP-β-CD, (B) HP-β-CD-PLA-DPPE (30:1), and (C) $^{13}$C NMR spectrum of the HP-β-CD, (D) HP-β-CD-PLA-DPPE (30:1).

Figure 2 shows the $^{1}$H NMR spectrum of HP-β-CD and HP-β-CD-PLA-DPPE copolymer. The characteristic absorption peaks are also indicated in the figure. Compared with HP-β-CD (Fig. 2A), the $^{1}$H NMR spectra of the HP-β-CD-PLA-DPPE copolymer (Fig. 2B) showed that the signal at ~0.9 ppm was attributed to the terminal methyl proton of the DPPE moiety. The signals at ~ 1.2, 1.3, 1.6, 3.1 and 3.3 ppm were attributed to the methenyl protons of $-CH_2$ group in DPPE moiety. The signal at ~ 5.2 ppm was assigned to the proton of −CH group in the PLA and DPPE moiety. The peak at ~8.3 ppm was attributed to the protons of the phosphate group in the DPPE moiety.

The basic chemical structure of HP-β-CD-PLA-DPPE copolymer is further confirmed by $^{13}$C-NMR (Figs. 2C and 2D). Compared with HP-β-CD (Fig. 2C), the$^{13}$C NMR spectra of the HP-β-CD-PLA-DPPE copolymer (Fig. 2D) showed that the peak at ~9.0 ppm was attributed to the $-CH_3$ group carbon peak of the DPPE moiety located at the terminal groups. The signals at ~19, ~ 30, ~ 42 and ~70 ppm were assigned to $-CH_2$ group carbon peak of the DPPE moiety. The signal at ~78 ppm was assigned to −CH group carbon peak of the DPPE moiety. The signal at ~170 ppm was assigned to −COO group carbon peak of the PLA and DPPE moiety. These above results evidenced that the copolymer contained DPPE side chains.

Furthermore, the typical $^{31}$P NMR spectra of DPPE and HP-β-CD-PLA-DPPE copolymer were recorded as shown in Figure 3. Compared with DPPE (Fig. 3a) (-1.22 ppm), the $^{31}$P NMR spectra of the HP-β-CD-PLA-DPPE copolymer (Fig. 3b) showed that the peak at 0.62 ppm was generally expected for $^{31}$P functionalities.[36,37] The $^{31}$P NMR spectra confirmed

 DOI 10.1002/jps

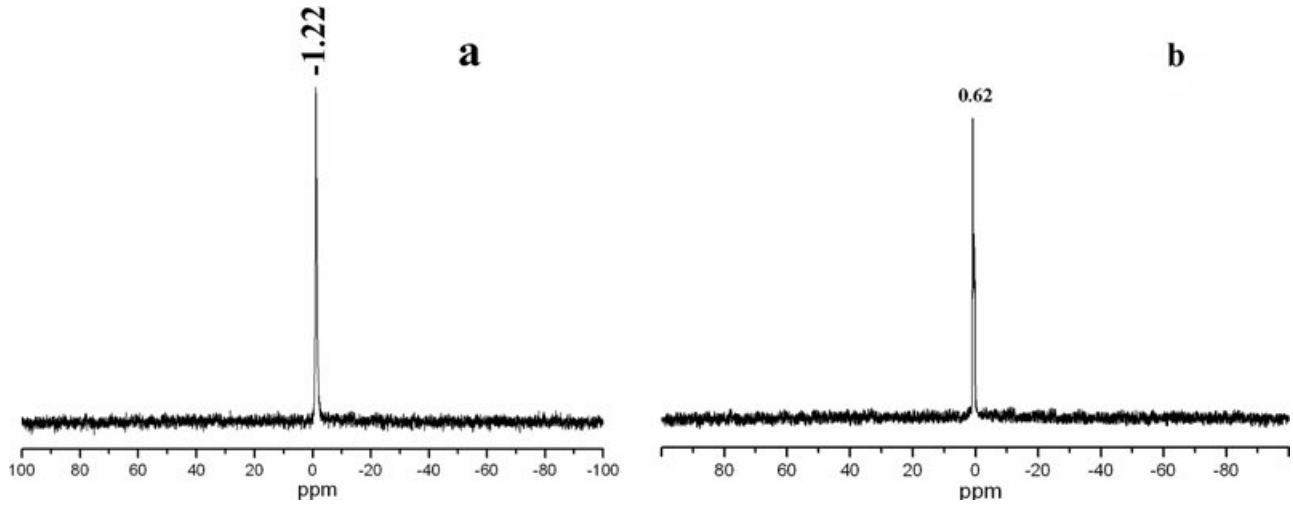


**Figure 3.** The typical $^{31}P$ nuclear magnetic resonance spectrum of (a) DPPE and (b) HP-β-CD-PLA-DPPE (10:1 ).

that phosphate groups were chemically bonded to the material.

Thermogravimetric (TG) curves of HP-β-CD, HP-β-CD-co-PLA, and HP-β-CD-co-PLA-DPPE copolymers are shown in Figure 4a. It could be seen that all of the copolymer samples exhibited a weight loss during the heating process. Compared with HP-β-CD, HP-β-CD-PLA and HP-β-CD-PLA-DPPE copolymers have lower thermal degradation temperature. A fast process of weight loss appeared in the TG curves response for the HP-β-CD-PLA-DPPE copolymers in thermal degradation ranges. These results also indicated that the thermal stability of the copolymer further decreased due to the introduction of DPPE chains.

The DSC of HP-β-CD, HP-β-CD-PLA and HP-β-CD-PLA-DPPE copolymers was measured and the representative DSC traces are shown in Figure 4b. Only one sidestep presented in all of the samples and it showed that there were no existence of inhomogeneities. The $T_g$ of the HP-β-CD is 88.9°C. The $T_g$ of the HP-β-CD-PLA and HP-β-CD-PLA-DPPE copolymers are far lower than that of pure HP-β-CD. The decrease in the $T_g$ of HP-β-CD after introduction of PLA and DPPE indicated that there is interaction between supermolecular HP-β-CD and PLA, and HP-β-CD-PLA and DPPE. The introduction of the DPPE group will further decrease $T_g$.

The plots of retained weight, in percentage versus time, are demonstrated in Figure 5. It indicated that the hydrophilicity–hydrophobicity balance plays an important role in the biodegradation of the HP-β-CD-PLA-DPPE copolymer. Because the HP-β-CD unit of HP-β-CD-PLA-DPPE copolymers is hydrophilic, water can diffuse into the copolymer matrix so that the

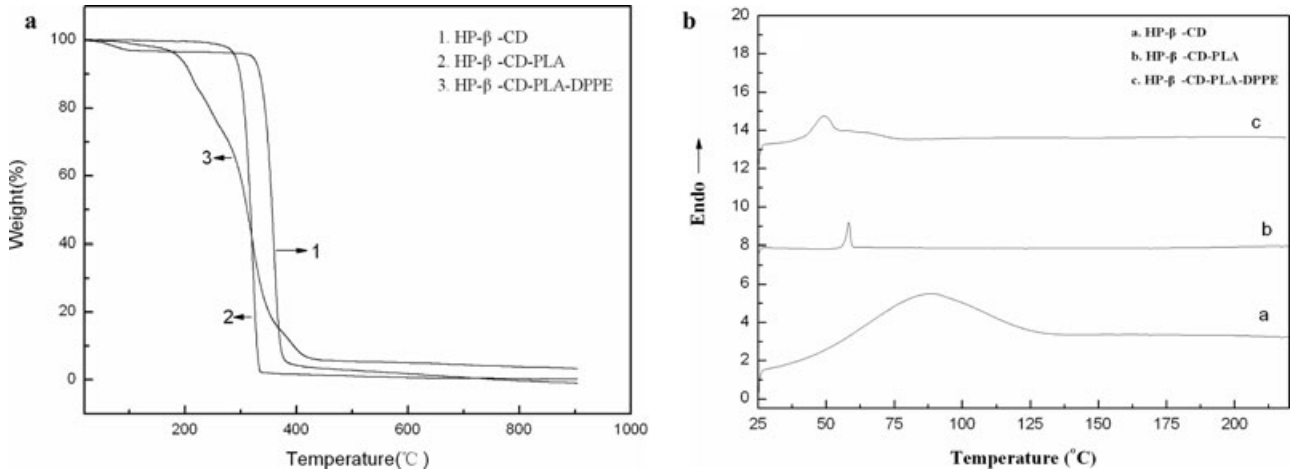


**Figure 4.** (a) Thermogravimetric analysis graphs of HP-β-CD, HP-β-CD-PLA, and HP-β-CD-PLA-DPPE (30:1) and (b) differential scanning calorimetry thermograms of HP-β-CD, HP-β-CD-PLA, and HP-β-CD-PLA-DPPE (30:1).

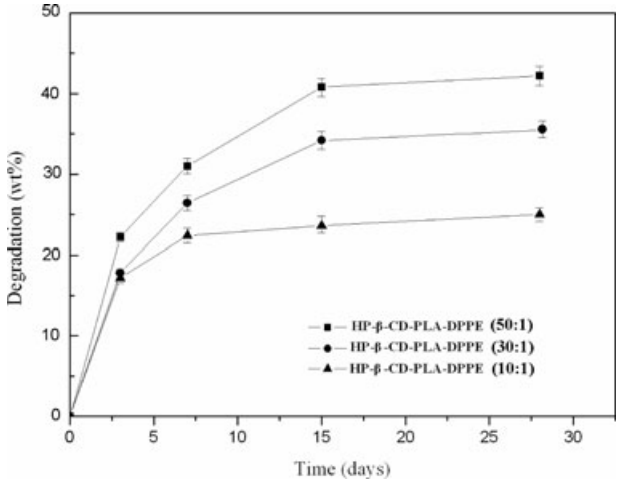


**Figure 5.** Weight Loss of the HP-β-CD-PLA-DPPE copolymers in PBS (pH 7.4) at 37°C.

biodegradation takes place simultaneously inside the copolymer disk and on its outer layer. In addition, the HP-β-CD-PLA-DPPE copolymers with small Mw are biodegraded with higher rate than those with high Mw. It could be explained by the fact that the polymeric chains of small Mw have better mobility and more hydrophilicity, so that it is easier for the water molecules to penetrate into the polymer matrix.

### Micelle Formation

The amphiphilic nature of the HP-β-CD-PLA-DPPE copolymer provides an opportunity to form micelles in water. The water-soluble HP-β-CD chains serve as the hydrophilic shell stabilizing the nanoparticle, and PLA and DPPE constitute the hydrophobic core. A pyrene probe is used to detect the micelle formation of HP-β-CD-PLA-DPPE and to measure its CMC. The microscopic characteristics of resultant amphiphilic copolymer in aqueous medium were investigated using a fluorometer in the presence of pyrene as a fluorescent probe. It is known that the variation in the ratio $I_1/I_3$ of intensity of first (372 nm) to the third (383 nm) vibronic peaks, the so-called polarity parameter, is quite sensitive to the polarity of microenvironment where the pyrene is located. Figures 6a and 6b showed the emission spectra of pyrene in its aqueous solutions with various concentrations and the change of $I_1/I_3$ with the concentration. At lower concentrations, the $I_1/I_3$ values remained nearly unchanged. With further increase of concentration, the intensity ratio begins to decrease, implying the onset of micelle from HP-β-CD-PLA-DPPE copolymer. The CMC was determined to be $6.47 \times 10^{-2}$ mg/mL by the interception of two straight lines. Compared with low Mw surfactants, the resultant amphiphilic copolymer has a lower CMC value, indicating the stability of the micelles from this HP-β-CD-PLA-DPPE copolymer at aqueous solution. Further work was carried out on the morphology of the formed micelles by the TEM technique. From Figure 7a, it can be confirmed that the resulting plain copolymeric micelles in water are spherical in shape, with the diameters ranging from 120 to 140 nm. The size distribution of the plain micelles was also investigated by the dynamic light scattering (DLS) technique. As shown in Figure 7b, a relative narrow size distribution was obtained.

### Formation of Dox-Loaded Nanoparticles

DOX-loaded HP-β-CD-PLA-DPPE copolymer NPs were fabricated by DE and NP methods. The copolymer composition has effect on the particle size of NPs. The higher content of DPPE segment resulted in particle size increase. The increased DPPE segment could

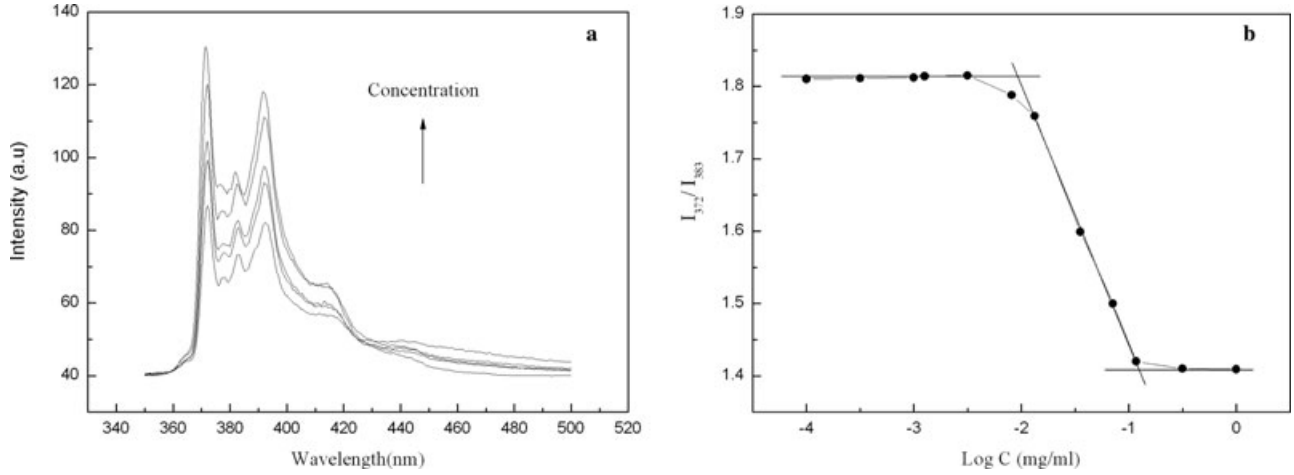


**Figure 6.** (a) Fluorescence emission spectra of pyrene in water in the presence of HP-β-CD-PLA-DPPE copolymer at 20°C (copolymer concentration 0.5, 0.01, 0.005, 0.001, 0.0001 mg/mL) and (b) change of the intensity ratio ($I_1/I_3$) versus the concentration of the HP-β-CD-PLA-DPPE copolymer at 20°C.

 DOI 10.1002/jps

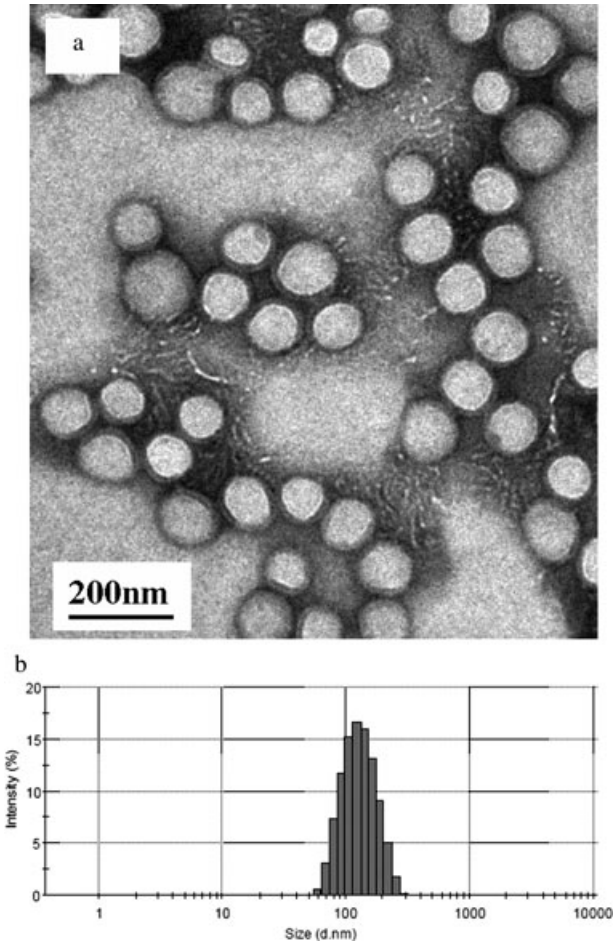


**Figure 7.** (a) Transmission electron microscope images of morphology of plain HP-β-CD-PLA-DPPE (30:1) micelles and (b) their size distribution determined by dynamic light scattering.

decrease the diffusion of DOX, which was in favor of EE enhancing. In addition, the interactions between DPPE and DOX were favorable for enhancing EE. It meant that the copolymer composition impacted greatly on EE. For above reasons, the EE of different samples increased with the increasing of ratio of DPPE. The EE% of DOX in the HP-β-CD-PLA-DPPE copolymer NPs was much improved in comparison with EE% of DOX in the corresponding PLA NPs (data not shown). The reasons for high EE% will be considered as follows. Firstly, the inclusion complexes may be formed from the accessible residues of DOX with the hydrophobic cavity of HP-β-CD moiety, because such inclusion complexes were easily formed from small organic molecules with free HP-β-CD.[33] The cavity size of HP-β-CD is suitable to bind DOX. Therefore, the formation of inclusion complexes was quite possible. Secondly, the interactions occurred between DOX and HP-β-CD-PLA-DPPE copolymer. Thirdly, the HP-β-CD-PLA-DPPE copolymer was amphiphilic so that its special structure was accessible to DOX molecule. All the effects contributed to the increased EE%. If the HP-β-CD moiety was helpful for the improvement of EE%, it was easy to understand why the HP-β-CD-PLA-DPPE copolymer NPs loaded more DOX. Of course, the better hydrophilic–hydrophobic balance of the HP-β-CD-PLA-DPPE copolymer must be important.

The nanoparticle diameters of HP-β-CD-PLA-DPPE copolymer were measured and data were collected in Table 2. In both methods, the nanoparticle diameter became smaller as the Mw of the copolymer HP-β-CD-PLA-DPPE decreased. A decrease in the Mw of the copolymer HP-β-CD-PLA-DPPE will result in an increase in its hydrophilicity–hydrophobicity balance. Because the surface tension was reduced with the increase of hydrophilicity, smaller NPs should be formed. The nanoparticle EE was also influenced by the fabrication technique. In the DE method, the EE was more than the NP method. This may be due to the different mechanisms for the nanoparticle formations in the two methods. The multinanoreservoir system was formed in the DE method while the single-layer nanosphere was fabricated in the NP method.

The morphology of DOX-loaded HP-β-CD-PLA-DPPE copolymer NPs is shown in Figures 8a and 8b. It could be confirmed that the NPs appeared to

**Table 2.** Effect of Material Composition on EE and Particle Size

| Method | Material Composition | EE (%) | Mean Hydrodynamic Diameter (nm) | PDI[a] | Zeta Potential (mV) |
|---|---|---|---|---|---|
| DE | HP-β-CD-PLA-DPPE (50:1) | 60.5 ± 2.3 | 141.6 ± 3.6 | 0.185–0.212 | −14.9 ± 1.3 |
| DE | HP-β-CD-PLA-DPPE (30:1) | 71.4 ± 1.7 | 152.3 ± 3.5 | 0.176–0.207 | −24.6 ± 0.9 |
| DE | HP-β-CD-PLA-DPPE (10:1) | 90.6 ± 0.8 | 182.1 ± 4.9 | 0.141–0.159 | −27.2 ± 2.5 |
| NP | HP-β-CD-PLA-DPPE (50:1) | 50.5 ± 2.4 | 131.4 ± 5.4 | 0.132–0.188 | −22.8 ± 1.8 |
| NP | HP-β-CD-PLA-DPPE (30:1) | 64.3 ± 1.1 | 141.7 ± 4.8 | 0.086–0.135 | −23.9 ± 2.1 |
| NP | HP-β-CD-PLA-DPPE (10:1) | 72.5 ± 1.9 | 166.2 ± 5.3 | 0.120–0.144 | −29.8 ± 1.9 |

[a] PDI represents polydispersity index.
EE, encapsulation efficiency.
DE, double emulsion.
NP, nanoprecipitation.
HP-β-CD-PLA-DPPE,hydroxypropyl-β-cyclodextrin-polylactide-1,2-dipalmitoyl-sn-glycero-3-phosphoethanolamine.

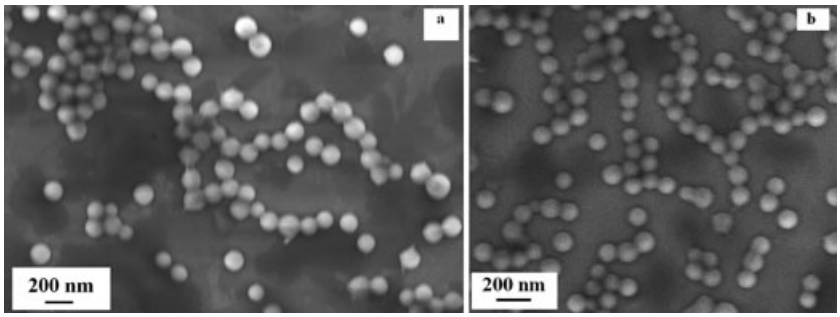


**Figure 8.** Scanning electron microscope images of DOX-loaded HP-β-CD-PLA-DPPE (30:1) nanoparticles fabrication by (a) double emulsion and (b) nanoprecipitation.

be spherical in shapes made by both NP and DE methods.

### *In Vitro* Drug Release Studies

Figure 9 shows *in vitro* release profiles of DOX from HP-β-CD-PLA-DPPE copolymer. For all NPs, DOX release showed both an initial burst and a release in a sustained manner afterward. This sustained release could result from diffusion of DOX into the polymer wall and through the polymer wall as well as erosion of the polymers. The maximal released amount is 80.13% for DE method and 91.25% for NP method in HP-β-CD-PLA-DPPE NPs, respectively.

It was noticed that different fabrication methods led to various release behavior. The released amount and rate of DOX from NPs with NP method was much faster than that of DE method. When the polymers are not soluble in water, drug molecules dissolved in water may be very close to the outer NPs surface, forming a layer of molecules, susceptible to be easily and rapidly released. In addition, more burst release was observed from NPs fabricated with NP technique than those from DE method. This was because different methods led to various distributions of DOX molecules in the NPs. The fabrication method determined the amount of drug existing near the surface of NPs. Using DE method, most DOX molecules were encapsulated within the NPs as the multinanoreservoir systems. Using NP method, NPs were formed as the multimolecular polymeric micelles trapping DOX molecules near their outer layers.

### Cellular Entry and Cytotoxicity of Nanoparticles-Encapsulated Doxorubicin

We sought to determine whether encapsulation of DOX in NPs would increase drug entry into tumor cells and cytotoxicity. Free DOX or NPs (NP or DE method) were added to cells cultured on 6-well plates such that DOX concentration was 1 μM, and after incubation for specific times, the cells were collected for

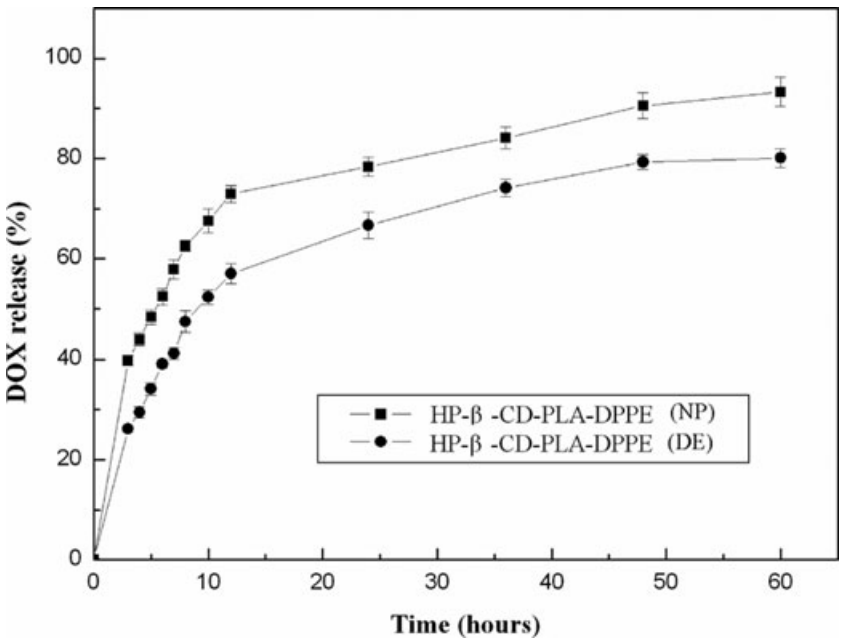


**Figure 9.** *In vitro* release profiles of DOX from the HP-β-CD-PLA-DPPE (30:1) nanoparticles.

 DOI 10.1002/jps

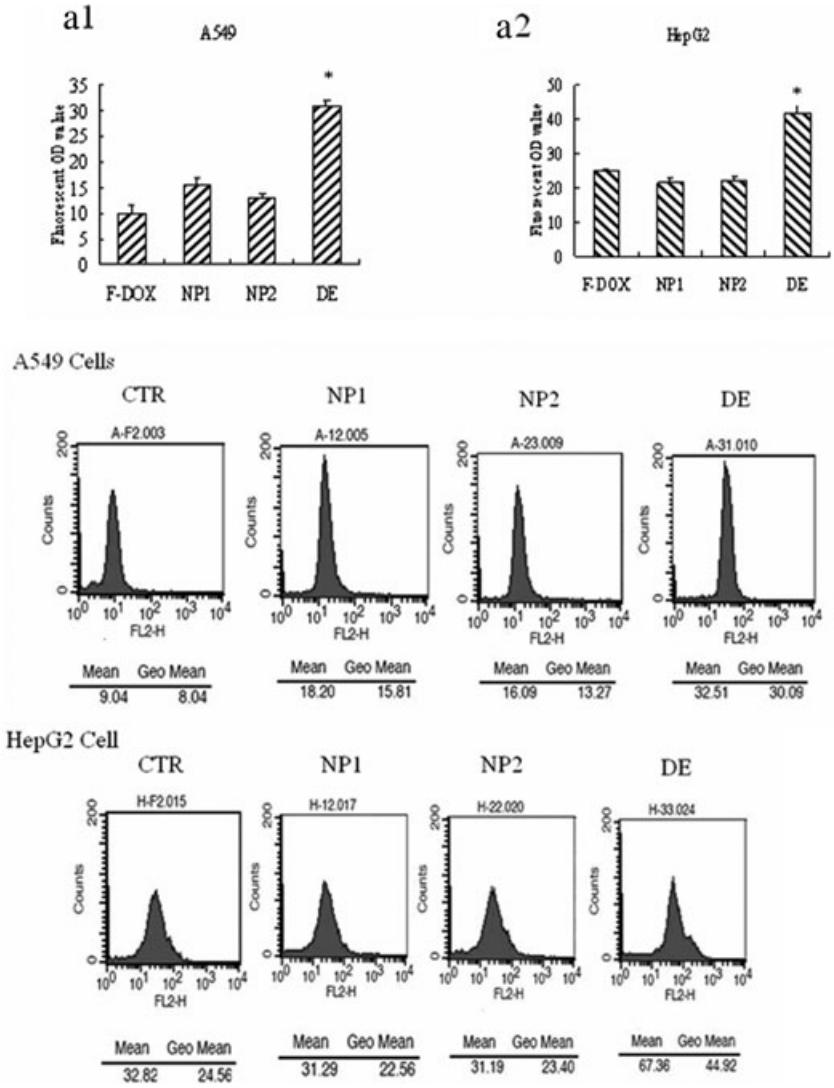


**Figure 10.** The flow cytometry analysis of free doxorubicin (DOX) and doxorubicin-loaded HP-β-CD-PLA-DPPE (30:1) nanoparticles (NP1 and DE were nanoprecipitation (NP) and double emulsion methods of HP-β-CD-PLA-DPPE (30:1), respectively; NP2 was NP method of HP-β-CD-PLA-DPPE (50:1); F-DOX was free DOX ).

analysis of DOX-derived fluorescence by flow cytometry.

DOX incorporated into NPs was more rapidly internalized than free DOX (Figs.10a1 and 10a2). Especially, fluorescence intensity significantly increased about three or twofolds compared to free DOX and NPs made by NP method, treated with NPs made by DE method in A549 cells and HepG2 cells.

To compare cytotoxic activity of encapsulated and free drug, tumor cells were exposed to a series of equivalent concentrations of free DOX or DOX encapsulated in NPs for 48 h, and the percentage of viable cells was quantified using the methylthiazoletetrazolium method. The concentration of DOX in nanoparticle, obtained by DE methods that caused 50% killing, was much lower than that of free DOX (Figs.11b1 and 11b2). These results indicate that the encapsulation of DOX in HP-β-CD-PLA-DPPE, used by DE methods, plays an important role in the enhancement of cytotoxic activity.

## CONCLUSION

A novel amphiphilic HP-β-CD-PLA-DPPE copolymer was synthesized. FT-IR, NMR, TGA, and DSC were used to investigate the physicochemical characteristics of the copolymer. The DOX-loaded copolymer NPs fabricated by DE and NP methods were proved having following properties: the bio-application of HP-β-CD and PE NPs and the enhancement of EE% of DOX during the released process. It was also shown that both copolymer composition and fabrication method obviously effect particle size and EE. *In vitro* antitumor activity of DOX-loaded NPs against

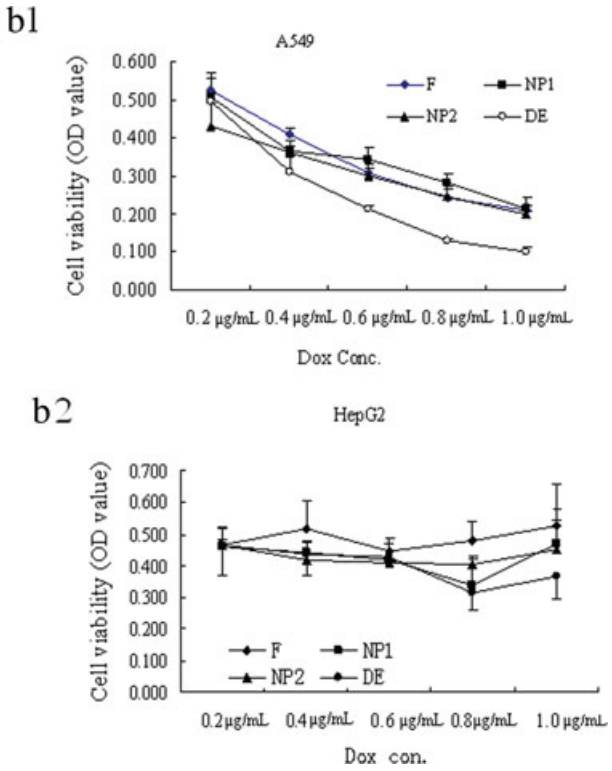


**Figure 11.** *In vitro* cytotoxicity of doxorubicin-loaded HP-β-CD-PLA-DPPE (30:1) nanoparticles against A549 and HepG2 (NP1 and DE were nanoprecipitation (NP) and double emulsion methods of HP-β-CD-PLA-DPPE (30:1), respectively; NP2 was NP method of HP-β-CD-PLA-DPPE (50:1); F-DOX was free DOX ).

cell was evaluated by 3-(4,5-dimethylthiazol-2-yl)-2,5-diphenyl tetrazolium bromide method. The results showed that DE method plays an important role in the enhancement of cytotoxic drug activity.

## ACKNOWLEDGMENTS

Project supported by the major program for fundamental research of the Chinese Academy of Sciences, China (no. KJCX2-YW-M02); the State Key Development Program for Basic Research of China (973) (no. 2009CB930200; 2010CB934004,2006CB933305), (863) (no. 2007AA02Z150).

## REFERENCES

1. Jones M, Leroux J. 1999. Polymeric micelles—a new generation of colloidal drug carriers. Eur J Pharm Biopharm 48:101–111.
2. Torchilin VP. 2001. Structure and design of polymeric surfactant-based drug delivery systems. J Control Release 73:137–172.
3. Savic R, Luo LB, Eisenberg A, Maysinger D. 2003. Micellar nanocontainers distribute to defined cytoplasmic organelles. Science 300:615–618.
4. Kwon GS, Okano T. 1996. Polymeric micelles as new drug carriers. Adv Drug Deliv Rev 21:107–116.
5. Shuai X, Merdan T, Schaper AK, Xi F, Kissel T. 2004. Core-cross-linked polymeric micelles as paclitaxel carriers. Bioconjug Chem 15:441–448.
6. Torchilin V. 2004. Targeted polymeric micelles for delivery of poorly soluble drugs. Cell Mol Life Sci 61:2549–2559.
7. Yuan F, Leunig M, Huang SK, Berk DA, Papahadjopoulos D, Jain RK. 1994. Microvascular permeability and interstitial penetration of sterically stabilized (stealth) liposomes in a human tumor xenograft. Cancer Res 54:3352–3356.
8. Gabizon AA. 2001. Pegylated liposomal doxorubicin: Metamorphosis of an old drug into a new form of chemotherapy. Cancer Invest 19:424–436.
9. Trubetskoy VS, Torchilin VP. 1995. Use of polyoxyethylene-lipid conjugates as long-circulating carriers for delivery of therapeutic and diagnostic agents. Adv Drug Deliv Rev 16:311–320.
10. Lukyanov AN, Gao Z, Mazzola L, Torchilin VP. 2002. Polyethylene glycol-diacyllipid micelles demonstrate increased acculumation in subcutaneous tumors in mice. Pharm Res 19:1424–1429.
11. Gao Z, Lukyanov AN, Singhal A, Torchilin VP. 2002. Diacyllipid-polymer micelles as nanocarriers for poorly soluble anticancer drugs. Nano Lett 2:979–982.
12. Gabizon AA. 1995. Liposome circulation time and tumor targeting: Implications for cancer chemotherapy. Adv Drug Deliv Rev 16:285–294.
13. Lukyanov AN, Elbayoumi TA, Chakilam AR, Torchilin VP. 2004. Tumor-targeted liposomes: Doxorubicin-loaded long-circulating liposomes modified with anti-cancer antibody. J Control Release 100:135–144.
14. Khan AR, Forgo P, Stine KJ, D'Souza VT. 1998. Methods for selective modifications of cyclodextrins. Chem Rev 98:1977–1996.
15. Uekama K, Hirayama F, Irie T. 1998. Cyclodextrin drug carrier systems. Chem.Rev 98:2045–2076.
16. Kang F, Singh J. 2003. Conformational stability of a model protein (bovine serum albumin) during primary emulsification process of PLGA microspheres synthesis. Int J Pharm 260:149–156.
17. Ionita G Ionita P, Sahini VE, Luca C. 2001. Influence of cyclodextrins on the kinetics of oxidation of amino acids and BSA by hydrazyl radicals. J Incl Phenom Macrocycl Chem 39:269–271.
18. Chiellini E, Solaro R. 2002. Contents of Macromolecular Symposia 1977th World Conference on biodegradable polymers and plastics, Tirrenia, Pisa (Italy). pp 345–354.
19. Soppimath KS, Aminabhavi TM, Kulkarni AR, Rudzinski WE. 2001. Biodegradable polymeric nanoparticles as drug delivery devices. J Control Release 70:1–20.
20. Peczuh MW, Hamilton AD. 2000. Peptide and protein recognition by designed molecules. Chem Rev 100:2479–2494.
21. Welbanks L. 2000. Adriamycin monograph .In: Compendium of pharmaceuticals and specialties Canadian Pharmacists Association, Ottawa, Canada. pp 31–32.
22. Chen Y, Burton MA, Codde JP, Napoli S, Martins IJ, Gray BN. 1992. Evaluation of ion-exchange microspheres as carrier for the anticancer drug doxorubicin: *In vitro* studies. J Pharm Pharmacol 44:211–215.
23. Lu JY, Lowe DA, Kennedy MD, Low PS. 1999. Folate targeted enzyme prodrug cancer therapy utilizing penicillin-V amidase and a doxorubicin prodrug. J Drug Target 7:43–53.
24. Hyon SH, Jamshidi K, Ikada Y. 1997. Synthesis of polylactides with different molecular weights. Biomaterials 18:1503–1508.
25. Xie DM, Yang KS, Sun WX. 2007. Formation and characterization of polylactide and β-cyclodextrin inclusion complex. Curr Appl Phys 7S1:e15–e18.
26. Li J, Chen B, Wang X, Goh SH. 2004. Preparation and characterization of inclusion complexes formed

by biodegradable poly(ε-caprolactone)-poly(tetrahydrofuran)-poly(ε-caprolactone) triblock copolymer and cyclodextrins. Polymer 45:1777–1785.
27. Onozuka S, Kojima M, Hattori K, Toda F. 1980. The regiospecific mono tosylation of cyclodextrins. Bull Chem Soc Jpn 53:3221–3224.
28. Nozaki T, Maeda Y, Ito K, Kitano H. 1995. Cyclodextrins modified with polymer chains which are responsive to external stimuli. Macromolecules 28:522–524.
29. Vandoorne F, Vercauteren R, Permentier D, Schacht E. 1985. Re-investigation of 4-nitrophenyl chloroformate activation of dextran. Evidence for the formation of different types of carbonate moieties. Makromol Chem 186:2455–2460.
30. Vandoorne F, Bruneel D, Schacht E. 1990. Effect of chemical modification of dextran on the degradation by dextranase. Bioact Compat Polym 5:4–15.
31. Axén R, Ernback S. 1971. Chemical fixation of enzymes to cyanogen halide activated polysaccharide carriers. Eur J Biochem 18:351–360.
32. Laakso T, Stjärnkvist P Sjöholm. 1987. Biodegradable microspheres. VI: Lysosomal release of covalently bound antiparasitic drugs from starch microparticles. J Pharm Sci 76:134–140.
33. Torchilin VP, Levchenko TS, Lukyanov AN, Khaw BA, Klibanov AL, Rammohan R, Samokhin GP, Whiteman KR. 2001. *p*-Nitrophenylcarbonyl-PEG-PE-liposomes: Fast and simple attachment of specific ligands, including monoclonal antibodies, to distal ends of PEG chains via *p*-nitrophenylcarbonyl groups. Biochim Biophys Acta 1511:397–411.
34. Rodrigues JS, Santos-Magalhaes NS, Coelho LCBB, Couvreur P, Ponchel G, Gref R. 2003. Novel core (polyester)-shell(polysaccharide) nanoparticles: Protein loading and surface modification with lectins. J Control Release 92:103–112.
35. Govender T, Stolnik S, Garnett MC, Illum L, Davis SS. 1999. PLGA nanoparticles prepared by nanoprecipitation: Drug loading and release studies of a water soluble drug. J Control Release 57:171–185.
36. Sabesan S, Neria S. 1992. Synthesis of glycosylphosphates and azides. Carbohyd Res 223:169–185.
37. Lebouc F, Dez I, Madec PJ. 2005. NMR study of the phosphonomethylation reaction on chitosan. Polymer 46:319–325.